J. Fluid Mech. (1967), *vol.* 30, *part* 1, *pp.* 21–31
Printed in Great Britain

Convection in horizontal layers with internal heat generation. Experiments

By D. J. TRITTON AND M. N. ZARRAGA
School of Physics, University of Newcastle upon Tyne

(Received 24 January 1967)

A largely qualitative experimental investigation has been made of cellular convection patterns produced by the instability of a horizontal layer of fluid heated uniformly throughout its body and cooled from above. The fluid was aqueous zinc sulphate solution, and the heating was produced by an electrolytic current. The flow was visualized and photographed using polystyrene beads which, because of a differential expansion, came out of suspension in regions where the fluid was hotter or colder than average.

The development of the cellular patterns as the Rayleigh number (a modified form) was varied was in many respects similar to that for Bénard convection. There were, however, two striking differences. First, the fluid descended in the centres of the cells and ascended at the peripheries; this was probably associated with the asymmetry between the heating and cooling. Secondly, and more surprisingly, the horizontal scale of the convection patterns was unusually large (except at the lowest Rayleigh numbers); the distance between rising and falling currents was observed to reach typically five times the depth of the layer.

This last observation may be relevant to theories of convection within the Earth's mantle, to mesoscale convection in the atmosphere, and to patterns formed in ice.

1. Introduction

Much attention, both experimental and theoretical, has been given to the convection of fluids between horizontal surfaces at different temperatures (often referred to as the Bénard configuration);† when the lower surface is the hotter, instability can bring the fluid into motion. The resulting flow pattern then consists of more-or-less regularly spaced rising and falling currents and thus one sees an array of 'convection cells' (unless the flow becomes turbulent). The long history of this subject is summarized in Stuart (1963, pp. 506–12) and Chandrasekhar (1961, chapter II). Recent experimental investigations, giving fairly full information about the various flow patterns, are those of Silveston (1958) (see also Schmidt & Silveston 1959) and Rossby (1966).

† This name persists although it is now believed that, in Bénard's experiments, the motion was driven by surface tension variations rather than by buoyancy (Pearson 1958). In the present paper we are concerned entirely with fluid layers between rigid boundaries, and therefore surface tension effects are irrelevant.

The present paper reports experiments on a configuration that is similar except that heat generation throughout the body of the fluid replaces heating from below. The heat leaves the fluid layer through the upper surface, so the stratification is again unstable.

A crude physical argument deriving from the discussion by Tozer (1965) led us to believe that this change would result in changes in the flow pattern. Suppose for a moment that it did not, and that familiar Bénard convection cells occurred with the usual size and structure. Heat is being generated everywhere within the fluid, and one may focus attention on that heat generated in regions where the velocity is zero (in the middle of the layer vertically and between the upgoing and downgoing currents horizontally). This heat will not be convected away. If the thermal conductivity is appropriately small—i.e. if the Rayleigh number and Prandtl number (see §2) are both sufficiently large—it will not be conducted away either. Hence, these regions must get steadily hotter and thus more buoyant, and in time the cellular pattern must be disrupted. Any steady convection pattern seems likely to be of a different structure, introducing temperature gradients large enough to counteract the effect of small conductivity (see also §5).

This argument gives little indication of the flow pattern that will occur. Our experiments aimed at finding this out.

To our knowledge there have been no previous laboratory experiments on convection with internal heat generation in arrangements in which the motion is due to instability rather than to the absence of an equilibrium configuration. On the theoretical side, Sparrow, Goldstein & Jonsson (1964) have developed the marginal stability theory for systems with internal heat generation, though with boundary conditions different from those of our experiments. Roberts (1967) has calculated the critical Rayleigh number for our case, and also applied to it his non-linear theory of the stability of one mode of convection with respect to another.

2. Specification of problem

The theoretical situation to which the experiments were intended to approximate consists of a layer of fluid of constant depth and infinite horizontal extent with heat being generated uniformly in it. The upper boundary is rigid and at a constant uniform temperature; the lower boundary is rigid and has no heat transferred through it (so that the vertical temperature gradient is zero there). These boundary conditions were chosen partly to correspond to those of a related geophysical problem (see §6), but this is also one of the simplest arrangements in which the matter discussed in §1 can be investigated.

It is well known that, subject to certain assumptions that are usually approximately fulfilled in the laboratory (the Boussinesq approximation), dynamical similarity for the Bénard configuration is specified by two non-dimensional parameters, the Rayleigh number and the Prandtl number. The former involves the temperature difference across the layer. In the present configuration, this is not imposed on the system, but is adjusted by the flow pattern; once convection

starts, it will fall below the value given by the parabolic conduction profile. Hence, a new form of the Rayleigh number bringing in the rate of internal heat generation has to be introduced. This is†

$$R = \frac{g\alpha H d^5}{\nu\kappa k} = \frac{g\alpha H d^5}{\rho C_p \nu \kappa^2},$$

where g is the acceleration due to gravity; H is the heat being generated per unit time and unit volume; d is the depth of the layer; and the remaining symbols are properties of the fluid (α, coefficient of expansion; ν kinematic viscosity; κ, thermal diffusivity (thermometric conductivity); k, thermal conductivity; ρ, density; C_p, specific heat).

The critical value of R for the boundary conditions given above, calculated by Roberts, is 2772 (denoted by R_c).

For all aspects other than the marginal stability, the Prandtl number,

$$P = \nu/\kappa,$$

is also a governing parameter of the present situation, just as in the Bénard case. The fluid used was water—as being the simplest in which to produce the internal heat generation (see §3)—and P was about 5·5 throughout the experiments.

The most serious cause of departure from the Boussinesq approximation was the temperature variation of viscosity.

3. Experimental arrangement

The apparatus was designed to approximate as closely as possible without undue complication to the theoretical arrangement specified in §2, subject of course to the need for either the top or the bottom to be transparent. The investigation was intended to be a qualitative one of the flow patterns and, as a matter of policy, little attention was given to detailed quantitative features.

The base of the apparatus consisted of a Perspex block, 4·5 cm thick, standing on three levelling screws. The side-walls of the convecting region rested on this block and a 'constant temperature plate' in turn rested on these. The Perspex block had a horizontal extent considerably greater than that of the convecting region and was fitted with walls to form a shallow tank; this arrangement enabled the constant temperature plate to be put on to the side-walls without trapping bubbles in the convecting region. Although the joins between the Perspex block and the side-walls and between the side-walls and the top plate were not sealed, liquid could be drained from the surrounding parts of the tank without removing that in the convecting region.

The side-walls formed an approximate square of side 29 cm. They were made of a mixture of Araldite and powdered aluminium (for a reason irrelevant to the present work); the aluminium was sufficiently thinly distributed that they were

† Our notation for the non-dimensional parameters has been chosen to correspond to that used by Roberts (1967). We suggest that, when it is desirable to distinguish them from parameters arising in other fluid dynamical problems, one should write Ra_H for R and Pr for P.

electrically insulating. Fixed along the inside of two opposite walls were zinc electrodes of the same height as the walls; leads ran out through the walls.

Because of the high power to which it appears in the Rayleigh number, there was little freedom in the choice of wall height (which was of course the depth of the convecting layer) for practicable temperature variations. Most of the results to be reported were obtained with 0·44 cm walls, a few with 0·7 cm walls.

The upper surface of the convecting layer was a copper plate with cooling water flowing in channels through it. To insulate this electrically from the convecting fluid, it was coated with a thin layer of polyurethane lacquer and then a thin layer of matt black paint; the latter gave a good background for the flow visualization method described below. The cooling water was supplied by a pump–thermostat unit at a rate of several litres per min. It flowed through thirteen parallel channels in the copper plate each 2·2 cm wide and separated by walls 0·3 cm thick; the thickness of copper between the channels and the coated bottom of the plate was 0·3 cm. The temperature of the cooling water was set to around 30 °C, and probably held constant to within about 0·1 °C.

The convecting fluid was aqueous zinc sulphate solution (about 5% by weight $ZnSO_4$). Its physical properties were taken as those of water. It was chosen to give a suitable electrical resistivity for the internal heat generation combined with a suitable density for the flow visualization (see below). The heat was generated ohmically by a 50 c/s alternating electrolytic current. The range of values of H (heat generation per unit volume) was 0·02 to 0·5 cal sec^{-1} cm^{-3}, and the total heat input varied between 30 and 800 watts. The precise extent of the temperature variations so produced is not known, but is estimated to have been about 8 °C for the largest heat input.

Redistribution of the current due to the skin effect will have been unimportant; the skin depth is around 10^4 times the depth of the layer. Any modification of the current by the motion will have been quite negligible; the magnetic Reynolds number is of the order of 10^{-9}.

On the other hand, the temperature field will have caused significant departures from uniformity in the heating; variations in the electrical resistivity of over 10% probably occurred at the highest value of R. The variation of mean temperature with height will have made H somewhat larger near the bottom of the layer than near the top. Horizontal variations of the temperature will similarly have resulted in variations in the heating, and there is thus a possible feedback mechanism of the flow on the heating. The relative stability of different modes can be very sensitive to effects like this. However, if high and low resistance regions are in series, maximum heating occurs in the former, whereas, if they are in parallel, it occurs in the latter. Hence the effect would be different for different orientations of the hot and cold regions relative to the electrodes. Since no such differences are to be observed in the flow patterns, one might infer that the effect is unimportant.

There are also potentially perturbing electromagnetic consequences of the non-uniform resistivity. Two effects have to be considered. First, the flow of an electric current in a direction in which the resistivity is changing gives rise to a space charge and thus to a body force on the fluid. Secondly, non-uniformities in

the current result in a redistribution of the forces between current elements in a way that might feed energy into the motion. In view of the unexpected nature of some of the results, it has been suggested to us that such effects might be influencing the flow. However, order-of-magnitude estimates can be made of the force produced by each of the effects, and it is, in both cases, about 10^{-5} times smaller than the buoyancy force produced by a similar temperature variation.

Visualization of the flow patterns was achieved using polystyrene beads with a typical diameter of 0·03 cm (and a small amount of wetting agent). The beads have a density of about 1·06 g cm^{-3}. They are often used in large-scale water flow experiments, where the very slow relative motion is unimportant. In small-scale experiments like the present, the beads would drop out of pure water too quickly. Hence, the density of the liquid has to be adjusted by dissolving controlled amounts of salt (in the present experiments this was being done in any case in connexion with the internal heat generation). The beads can then be got into permanent suspension. However, the situation is further complicated—though in a most useful way—by the fact that the beads have a smaller coefficient of expansion than water. A change in temperature thus makes the suspension no longer permanent. Hence, conditions in a convecting system can be adjusted so that beads fall out of the hot rising currents and rise out of the cold falling currents. This provides a particularly good method of flow visualization for experiments like the present, in which steady flow patterns in a layer of small vertical extent are being studied. One gets information from beads deposited on the bottom below hot regions, beads deposited on the top above cold regions, and beads still in suspension and thus following the flow. The last provides confirmation that the interpretation is correct, whilst the first two give both a better immediate impression and a better permanent record of the flow patterns. Further details will be provided by the presentation of the results in the next section.

4. Experimental observations

The results consist of observations of the flow patterns in the range between the onset of convection and the onset of turbulence. The flow patterns vary quite a lot over this range, and the results give a clear indication of this sequence of events. Because the work was intentionally a qualitative first investigation, they give less indication of the values of R at which the various observations were made. The conditions of each observation were, of course, metered, and we quote a value of R/R_c for each of the pictures. However, these figures should be regarded as rather rough estimates (because of: the high power to which d, not accurately known, appears in R; the rapid variation of α and ν with temperature; some discrepancy between observed resistivities and ones taken from tables; a tendency for the convection pattern to lock on to the deposited beads, when these had become numerous). The value of R_c used is the theoretical one.

Figures 1 to 11, plates 1 to 6, are photographs, taken with the camera directly below the convecting layer, of patterns formed as described in §3. All the figures are to the same scale; the field of view is almost the full horizontal extent of the

convecting layer.† The electrodes are on the sides just beyond the top and bottom of each picture.

Figures 1 to 9 are of flow patterns with the 0·44 cm walls; figures 10 and 11 are with the 0·7 cm walls. The scale, relative to the depth of the layer, is indicated by the white square printed on to the top right-hand corner of each picture; the side of this is equivalent to *twice* the depth of the layer.

In all these pictures the most evident feature is the polystyrene beads deposited on the bottom. Whether most of the beads go to the top or to the bottom depends of course on the mean density of the fluid. A fine adjustment to this can be made by varying the temperature of the cooling water in the upper boundary, and this was usually done to bring the majority of the beads to the bottom; experience revealed that the flow patterns were such that this showed them best. Some of the pictures also show small quantities of beads deposited on the top; one cannot discern which are which in the photographs, but this is, of course, easily seen in the apparatus itself, and the figure captions give this information.

The total number of beads deposited depends of course on how long the flow has been established before the photograph was taken (e.g. figures 3 and 4 are different views of similar physical situations). When the temperature differences are small one does not so readily observe the stage when beads have settled out just from the very hottest parts of the upgoing currents (as has been done in figures 4 and 5). Relative differences in the number of beads deposited in different places may be significant—a remark particularly relevant to figures 8 and 9.

A long exposure photograph may show additionally the streaks formed by the trajectories of beads still in suspension. This effect is shown particularly well by figure 5, and figures 4, 8, 10 and 11 are also longer exposures than the remainder. They show the horizontal flow between the rising and falling currents. A still photograph does not distinguish between the beads moving from the former to the latter near the top and those moving the opposite way near the bottom, but again actual observation can of course distinguish. The interpretation that the beads deposited on the bottom are below rising currents and those on the top are above falling ones is confirmed by the motion of beads still in suspension.

All the observations were made with R considerably above its critical value and so no attempt was made to verify the predictions of marginal stability theory. Even if the imprecision of the present work were removed, it is doubtful if the method would be suitable for this purpose; as the convection becomes weaker, the effect on the polystyrene beads becomes less marked, and the difference between a very weak motion and no motion at all would not be discernible.‡

† Small displacements may make variations in the proximity of individual sides of the layer to the corresponding sides of the photographs. Edge influences on the convection pattern can be seen in some cases (e.g. the right-hand side of figure 5, plate 3).

‡ The matter of the flow patterns at lower values of R/R_c assumes more importance in view of the theoretical work of Roberts (1967), in particular the implication of his figure 7 that there are no stable hexagonal patterns when $R/R_c < 3{\cdot}2$ (for a slightly different Prandtl number). We have no observations to compare with this. On the other hand, some of our observations are obviously in disagreement with the theory in that they correspond to points to the left of the left-hand limb of Roberts's figure 7. Hence, we do not necessarily expect to find a change away from the hexagonal patterns as R/R_c is decreased below 3·2. Further experiments are indicated.

Figures 1 to 8 show the sequence of events as R is increased. The patterns are in many ways characteristic of ones produced by instability and provide encouraging evidence *a posteriori* that the apparatus was behaving as required.

Nevertheless, in two ways the flow patterns differ strikingly from those observed in the Bénard configuration. The first is the direction of circulation in the convection cells. The fluid is rising at the peripheries of the cells and falling at the centres—the opposite way round from Bénard convection in water. Even at the higher R-values, when the pattern changes from an array of polygons to an array of 'rolls' (see below), the distinction is maintained; the upgoing currents still form a linear pattern whilst the downgoing ones are in separated local regions.

The second difference concerns the horizontal length-scale of the convection patterns. It can be seen that the size of the cells increases markedly as R is increased. Separations of around five times the depth of the layer between the centre of an upgoing region and the centre of a downgoing one become predominant in the cellular array. We refer to this as 'elongation' of the cells. Nothing similar has ever been observed with the Bénard configuration in the laboratory; there the distance between the upgoing and downgoing currents is always not very different from the depth of the layer.

For comparison, figure 9 shows cells of about the usual size. This pattern was obtained in our apparatus by a sudden considerable reduction in the temperature of the upper surface (with the internal heat generation switched off). The transient situation is poorly defined, but a roughly linear conduction profile perhaps occurs as a large amount of heat is removed from the system (including the upper parts of the Perspex base). The observed flow resembles the internal heat generation case in the direction of circulation but Bénard convection in the horizontal length-scale. Contrast between figure 9 and figures 1 to 8 is the most dramatic way of showing the elongation.

Despite the differences in direction of circulation and horizontal scale, the development with increasing Rayleigh number is in other ways similar to that for Bénard convection. This is true of the shape of the cells. For the lower R values, they are polygonal with hexagons predominating. Figures 4 and 5 show this particularly well. Figure 6 may be regarded as showing a transition stage; and in figures 7 and 8 the pattern is more of a 'roll' type. There are signs, however, that the rolls are segmented into quadrilaterals. True rolls consist of parallel and similar lines of rising and falling currents, and these are observed in Bénard convection (though they are seldom completely straight). In our experiments, the strongest upgoing currents approximate to parallel lines, but there are other upgoing currents in lines roughly at right angles; these are presumably at a lower temperature, as fewer beads deposit from them. The downgoing currents are localized within the quadrilaterals and thus do not form a linear pattern as they would in true rolls.

This is a development that is not wholly paralleled in Bénard convection. However, some of Silveston's (1958) photographs do show patterns intermediate between hexagonal and roll types, in which some sides of the hexagons are weaker than others. And Rossby (1966) observed rolls with a length-wise periodic triangular structure.

The 'roll/quadrilateral' pattern shows the elongation to about the same extent

as the largest polygonal pattern, without much variation with R. The weaker upgoing currents are closer together than the stronger.†

Figures 10 and 11 show results obtained with the 0·7 cm walls; the former is for comparison with figure 8, the latter to extend the R range. Elongation again occurs but not to the same extent; i.e. the horizontal scale is not increased in proportion to the vertical. This is perturbing, but is probably a consequence of the finite horizontal extent of the apparatus (the elongation was not anticipated). The total number of cells is not large, and edge effects could extend to the middle. (If this explanation is correct, the remark above about the elongation not increasing much at higher R values is of little significance.) One other way in which a departure from similarity requirements could come about is the smaller temperature variation and hence smaller viscosity variation for larger d at the same R.

The flow pattern at high R/R_c shown in figure 11 is again a roll/quadrilateral pattern. However, the downgoing currents are beginning to be longer parallel to the lines of strong upgoing currents than perpendicular to them. The persisting localization might look less marked if a higher proportion of the beads were deposited on the top, but the geometrical difference between upgoing and downgoing currents would evidently remain.

The value of R of figure 11 is about the highest at which a cellular pattern can be observed. For higher values, the motion is turbulent. Beads in suspension can be observed to follow quite irregular trajectories. The transition to turbulence is not well specified in the Bénard case, and the Rayleigh number assigned to it is very variable (Willis & Deardorff 1965). In the present experiments, suspended beads could sometimes be observed to move in an irregular way (locally but not usually everywhere) whilst other beads were being deposited in a definite pattern. In both cases there appears to be a long transition between the first appearance (as the Rayleigh number is increased) of some irregularities and the disappearance of all regularities. In the present experiments it may also be that the deposition of the beads has a stabilizing effect on the patterns. Despite these comments, it is probably valid to conclude that the flow remains non-turbulent to values of R/R_c high compared with the corresponding ratio of Rayleigh numbers for the Bénard configuration (at comparable P).

5. Discussion

The two features of the observations that raise questions not previously raised are the direction of circulation and the elongation.

Roberts (1967) finds that all hexagonal convection patterns with the fluid rising at the cell centres are unstable. This may be considered a partial explanation of our results, but not a complete one as some of the patterns that we do observe are also unstable according to his theory (see below).

Without the aid of a full theory, we anticipated from physical considerations the reversal compared with Bénard convection in water; the following is an out-

† The difference in strength and the difference in separation are presumably related. Fluid travelling a shorter distance horizontally may have less time to heat.

line of the reasoning. In the Bénard case, the direction of circulation depends on whether the viscosity increases or decreases with increasing temperature (Tippelskirch 1956; Palm 1960; Segel & Stuart 1962). That is a situation such that, if gravity is reversed and heating and cooling are interchanged, the original situation is restored. Then, if one ignores the temperature variation of viscosity, flow patterns similar except for the direction of circulation must, from symmetry considerations, be equally probable. The present configuration does not have this symmetry, and the direction of circulation may in principle be determinate on the Boussinesq approximation with constant viscosity. It is probably determined by the fact that the fluid is being heated over a volume and cooled at a surface. Only fluid that has been relatively close to the upper surface can lose much heat by conduction out of the system, whereas all the fluid is being heated continuously. Thus one may expect the regions colder than average to be strong and localized and those hotter than average to be weak and diffuse. [This stage of the argument is evidently somewhat intuitive, but may be supported by reference again to Bénard convection and, in particular, to the type of flow of which figure 8 of Fromm (1965) is an example. In this the temperature distribution consists of comparatively narrow hot and cold plumes originating in the thermal boundary layers on respectively the lower and upper surfaces, with approximately isothermal regions in between. In the internal heat generation configuration the production of the cold downgoing plumes can occur in much the same way, but there will be no thermal boundary layer on the bottom and so no mechanism to form narrow regions of fluid much hotter than average.] When the cold regions are at the centres of the cells, they will be stronger and narrower than the hot regions. This may be illustrated by figure 7*b* of Chandrasekhar (1961), which shows that for a single wave-number hexagonal pattern the total amount of fluid enclosed in the centres of cells by zero vertical velocity curves is much less than that outside. The isotherms would form an identical pattern. The pattern will not be a single wave-number one when the thermal boundary layer is clearly formed, but the more general case most likely shows the same feature.†

Of course, viscosity variation could have an effect on the flow with internal heat generation if it were large enough, and indeed the present experiments do involve a significant variation. On the basis of the observations, however, it is not large enough to counteract the effect discussed above.‡

The elongation is much more surprising than the circulation reversal. Predictions of cell size are given both by marginal stability theory (Sparrow, Goldstein

† That it does so is suggested by the success of the temperature variation of viscosity theory in accounting for the direction of circulation in the Bénard situation. A way of viewing this physically is to suppose that the flow adjusts to make the viscosity smaller where the shear is larger.

‡ It should perhaps be noted that there could be an interaction between the temperature variation of electrical resistivity and the direction of circulation. A flow with the hotter fluid at the cell peripheries produces a continuous network of lower-resistance regions that is not produced by the reverse flow. This would result in a slightly lower total resistance and slightly greater total heating. However, there is not necessarily any reason why the flow should adjust to bring this about. Also the change in the total resistance on changing the geometry is second order in the resistivity variations.

& Jonsson 1964; Roberts 1967) and by non-linear stability theory (Roberts 1967). Neither gives any reason for expecting the elongation. There is, however, no contradiction between our observations and the marginal theory; the former show the elongation increasing as R is increased, and extrapolation backwards suggests that for $R/R_c \sim 1$ the distance between rising and falling currents would be much the same as the depth of the layer. On the other hand, there is clear disagreement with Roberts's non-linear theory, in that this indicates that hexagonal cells of the size observed are unstable. Presumably the assumptions of the theory are in some unknown way not applicable to our experiments.

In the absence of rigorous theory, one would like some physical understanding of the elongation, although, since it was quite unpredicted, this must be 'rationalization after the event'. The reason given in §1 for expecting differences from Bénard convection—the question of how the heat generated where the fluid is stationary is removed—should be relevant here. At first sight the observed behaviour poses this problem just as much; indeed the volume of each region where heat seems to accumulate appears to be increased. The resolution of this difficulty is perhaps contained in the following consideration. The elongated cells provide an altogether very inefficient heat transfer mechanism. Continuity requires that horizontal components of the velocity will be large compared with the vertical. The viscous forces that oppose these horizontal motions must be balanced by pressure forces. The horizontal pressure distribution will be different at different depths and thus involve vertical pressure gradients, which, because of the difference in length-scales, will be large compared with the horizontal gradients. This implies that the buoyancy force is mainly opposed by pressure forces, and that the vertical components of the viscous and inertial forces *must* be comparable with only a small part of the buoyancy force. The elongation thus makes the vertical velocities smaller than they would be for comparable buoyancy forces and no elongation. It is, of course, the vertical velocities that convect heat up towards the cold surface. Since the heat input is specified, the mean temperature difference across the layer must be increased by the elongation. The vertical temperature gradients may remain large enough for heat to be conducted away from the stationary regions whilst the temperature in these remains less than in the rising regions. In short, when there is elongation, the convection modifies the temperature field from a purely conduction situation relatively little.

6. Possible applications

Our interest in convection with internal heating was stimulated by discussions of the hypothesis that the Earth's mantle is convecting. A likely source of energy for this is radiogenic heating within the mantle itself. Our results are relevant to this in view of the controversy about how much of the mantle may be in motion. Many points of view have been expressed, but here we may oversimplify by considering just two. Models such as Runcorn's (1962) show convection extending throughout the mantle, whereas Tozer (1965) and others have argued that convection may be confined to a relatively small upper part of the mantle. A

powerful argument for the former point of view has seemed to be provided by the fact that the horizontal scale of the surface features that might be manifestations of the convection is comparable with the depth of the whole mantle. If elongated cells can occur, this argument loses its force, and thus, at least in a negative sense, our experiments support the second point of view.

Photographs of cloud patterns from satellites have revealed atmospheric convection patterns on a scale previously unobservable. Some of these patterns are distinctively cellular and have a horizontal scale large compared with the depth of the unstable layer (Krueger & Fritz 1961, Hubert 1966). It is not evident that body heating or cooling plays any major role in these, although they could be introduced by radiative transfer or by evaporation and condensation. It may be that the explanation is quite different, such as the anisotropy of small-scale turbulence (Hubert (1966) has developed a somewhat detailed theory of this). Nevertheless, it is interesting to note these observations in the present context, since the elongation of the atmospheric cells has hitherto seemed to be in sharp contrast with laboratory observations.

Elongated cells have also been reported in connexion with the patterns formed in pond ice (Woodcock & Riley 1947), and similar comments may be made about these.

We are much indebted to Dr D. C. Tozer for interesting discussions both before and during the work and to Dr C. W. Titman for helpful suggestions about the experiments.

REFERENCES

CHANDRASEKHAR, S. 1961 *Hydrodynamic and Hydromagnetic Stability*. Oxford University Press.

FROMM, J. E. 1965 *Phys. Fluids*, **8**, 1757.

HUBERT, L. F. 1966 *U.S. Dept. of Commerce, Environmental Science Services Administration, Meteorological Satellite Laboratory, Rept.* no. 37.

KRUEGER, A. F. & FRITZ, S. 1961 *Tellus*, **13**, 1.

PALM, E. 1960 *J. Fluid Mech.* **8**, 183.

PEARSON, J. R. A. 1958 *J. Fluid Mech.* **4**, 489.

ROBERTS, P. H. 1967 *J. Fluid Mech.* **30**, 33.

ROSSBY, H. T. 1966 *Mass. Inst. Tech., Dept. Geol. Geophys., Sci. Rept.* HRF/SR 27.

RUNCORN, S. K. 1962 *Nature, Lond.* **193**, 311.

SCHMIDT, E. & SILVESTON, P. L. 1959 *Chem. Engng. Prog., Symposium Series, Heat Transfer*, **55**, 163.

SEGEL, L. A. & STUART, J. T. 1962 *J. Fluid Mech.* **13**, 289.

SILVESTON, P. L. 1958 *Forsch. Geb. IngWes.* **24**, 29, 59.

SPARROW, E. M., GOLDSTEIN, R. J. & JONSSON, V. K. 1964 *J. Fluid Mech.* **18**, 513.

STUART, J. T. 1963 Hydrodynamic Stability, Sect. IX of *Laminar Boundary Layers* ed. by L. Rosenhead. Oxford University Press.

TIPPELSKIRCH, H. VON 1956 *Beitr. Phys. Atmos.* **29**, 37.

TOZER, D. C. 1965 *Phil. Trans.* A **258**, 252.

WILLIS, G. E. & DEARDORFF, J. W. 1965 *Phys. Fluids*, **8**, 2225.

WOODCOCK, A. H. & RILEY, G. A. 1947 *J. Met.* **4**, 100.

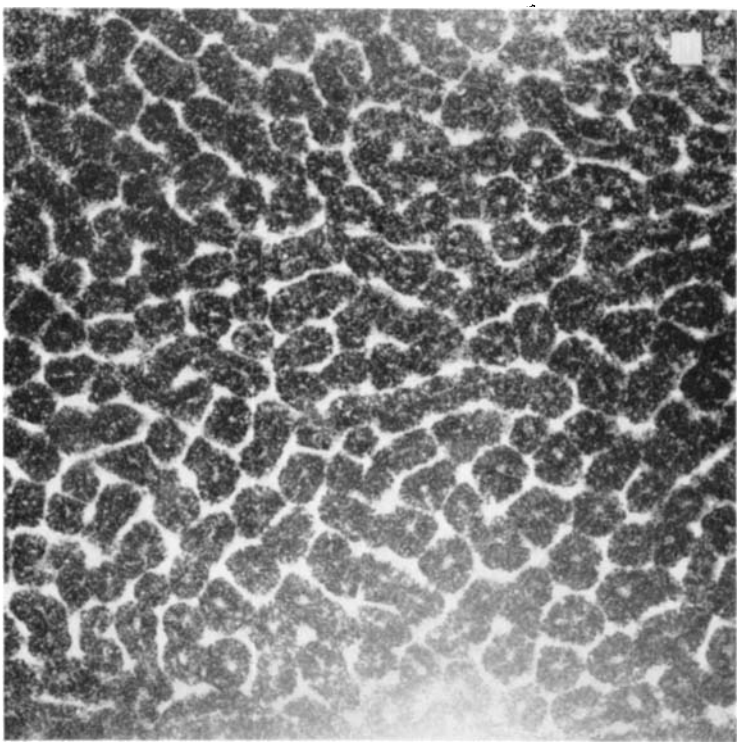

FIGURE 1. Convection pattern at $R/R_c \sim 4$. Most of the deposited beads are on the bottom; a few can be seen on the top at some of the cell centres.

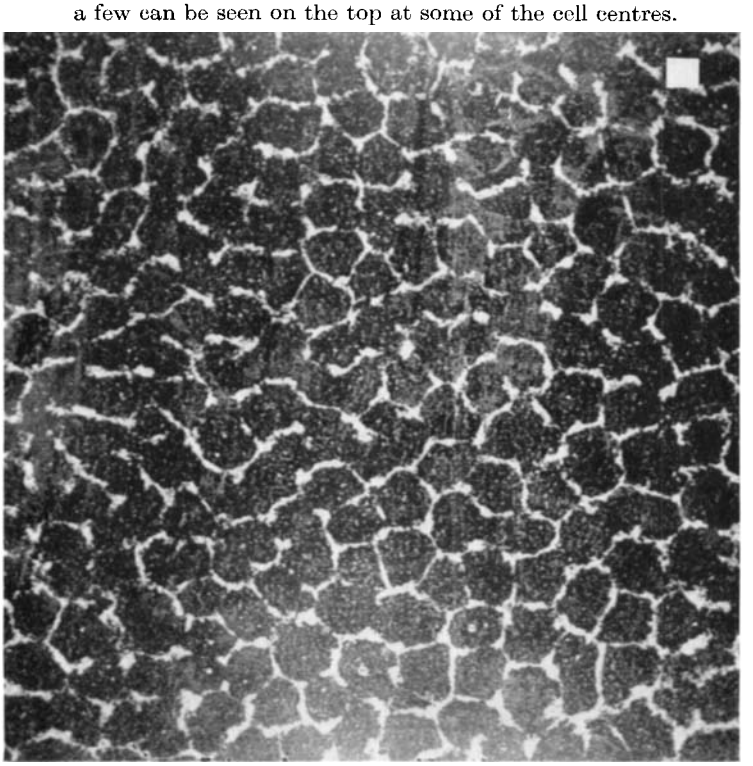

FIGURE 2. Convection pattern at $R/R_c \sim 7$, showing principally beads deposited on the bottom.

The scale of each figure is indicated by a white square in the top right hand corner. The side of this is equal to twice the depth of the layer.

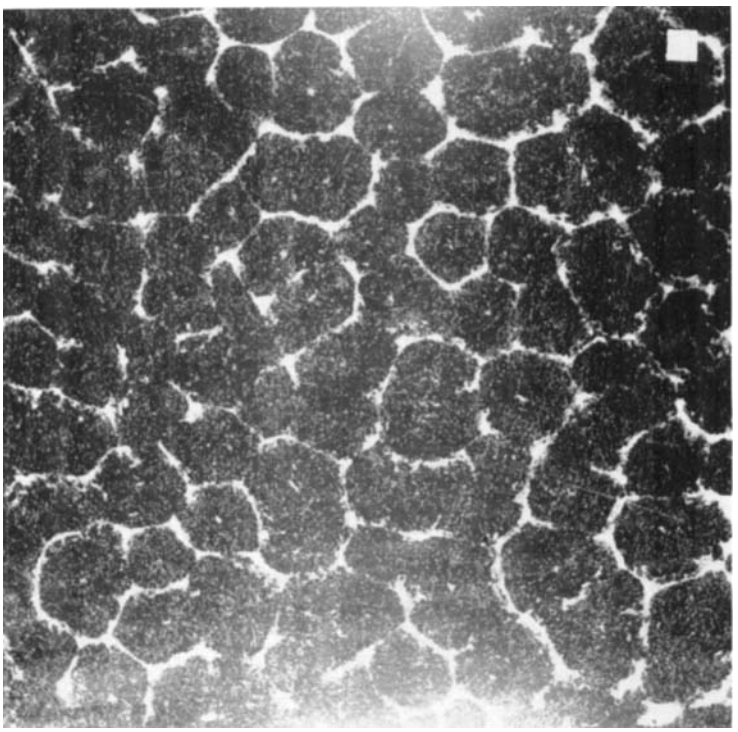

FIGURE 3. Convection pattern at $R/R_c \sim 9$, showing beads deposited on the bottom (and a very few on the top) and beads still in suspension (short exposure).

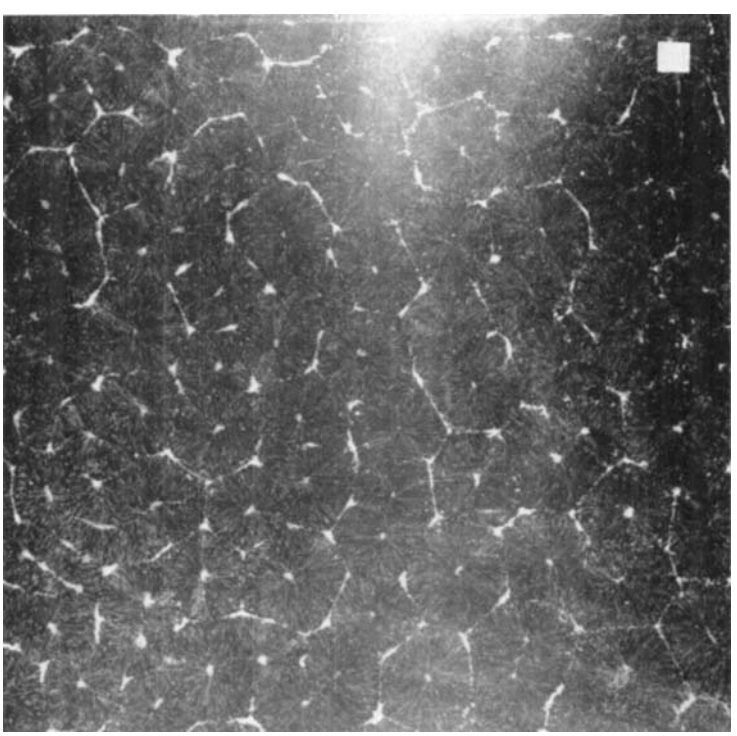

FIGURE 4. Convection pattern at $R/R_c \sim 10$. This is a long exposure showing streaks produced by the motion of beads still in suspension. Also seen are the polygonal pattern of beads deposited on the bottom and dots produced by beads deposited on the top.

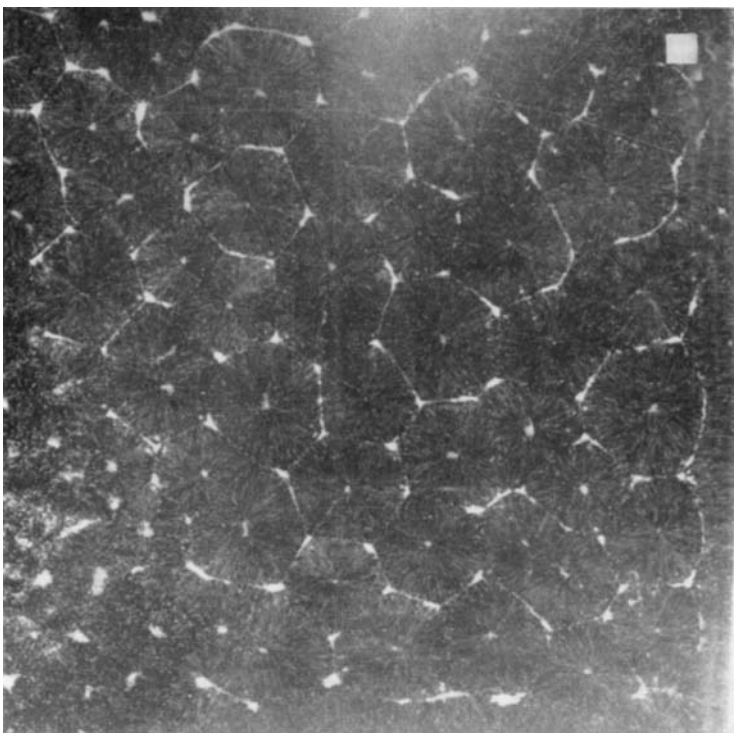

FIGURE 5. Convection pattern at $R/R_c \sim 15$. Interpretation as for figure 4.

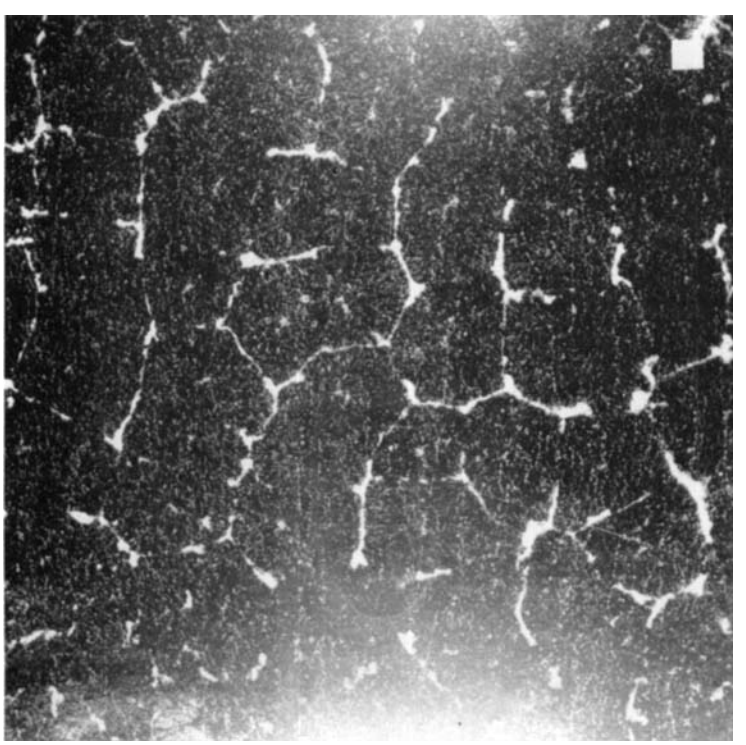

FIGURE 6. Convection pattern at $R/R_c \sim 30$, showing principally beads deposited on the bottom.

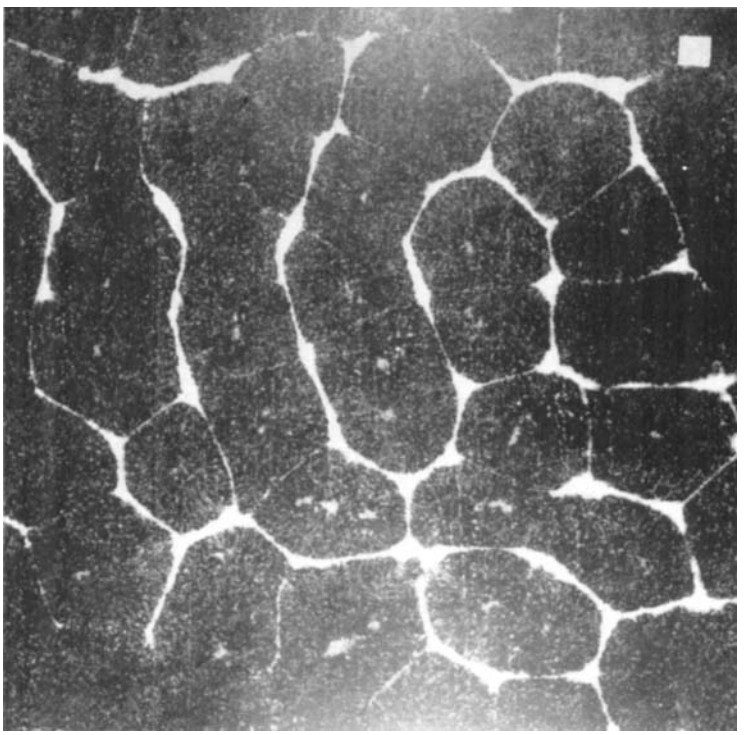

FIGURE 7. Convection pattern at $R/R_c \sim 40$. The main pattern is formed by beads deposited on the bottom; the faint lines are also beads deposited on the bottom, whilst the isolated dots are beads deposited on the top.

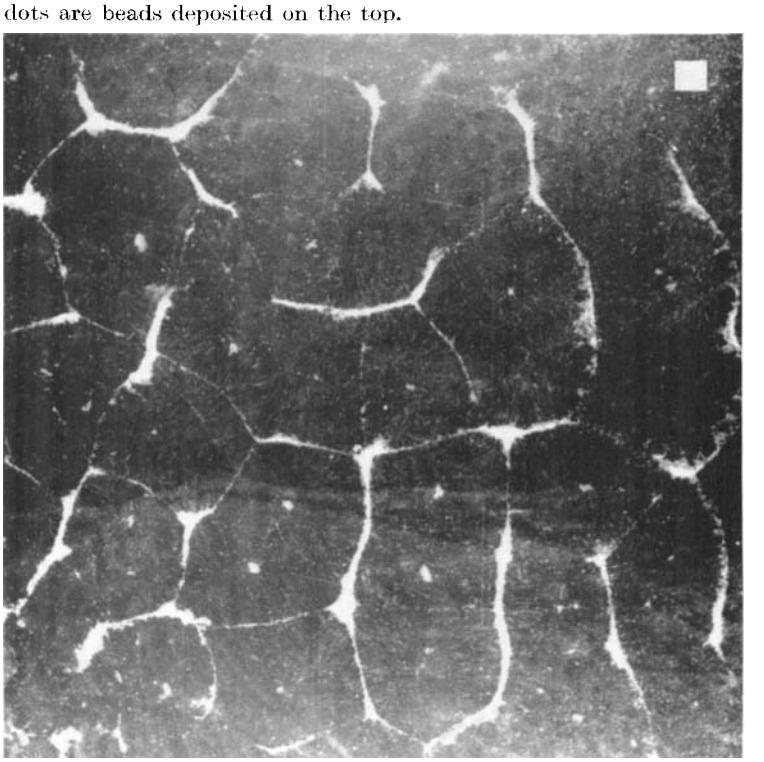

FIGURE 8. Convection pattern at $R/R_c \sim 45$. Interpretation is as for figure 7, except that figure 8 is a longer exposure and some streaks formed by beads still in suspension are to be seen.

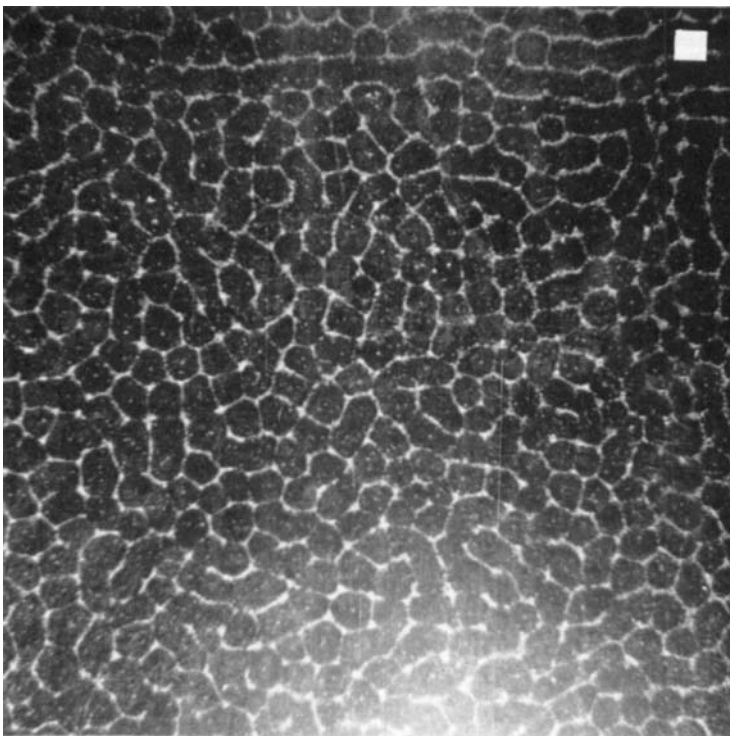

FIGURE 9. Pattern formed on the bottom when the temperature of the top plate is suddenly substantially reduced.

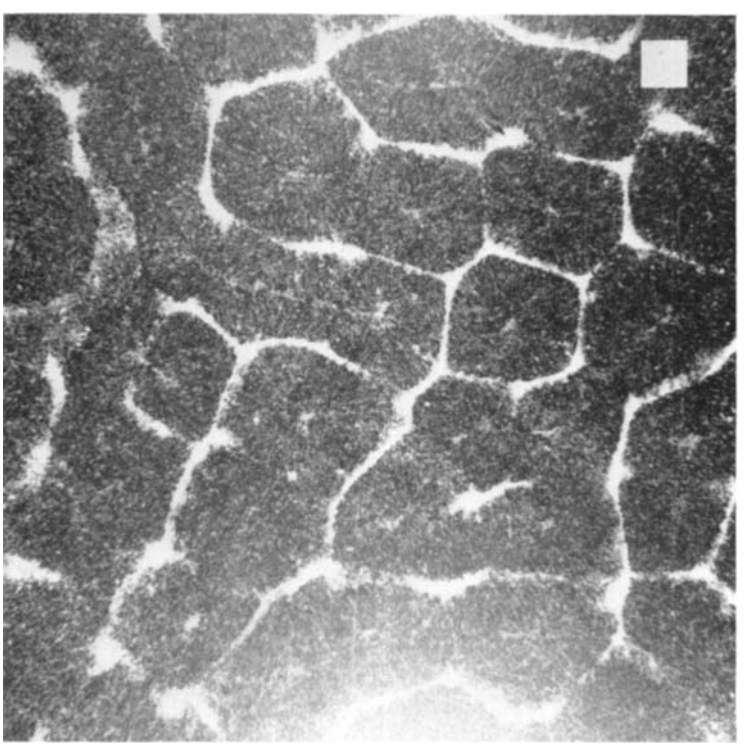

FIGURE 10. Convection pattern at $R/R_c \sim 45$ (with larger layer depth than that for figure 8), showing principally lines of beads on the bottom. Also to be seen are a few faint dots and one faint line of beads on the top, and streaks produced by beads still in suspension.

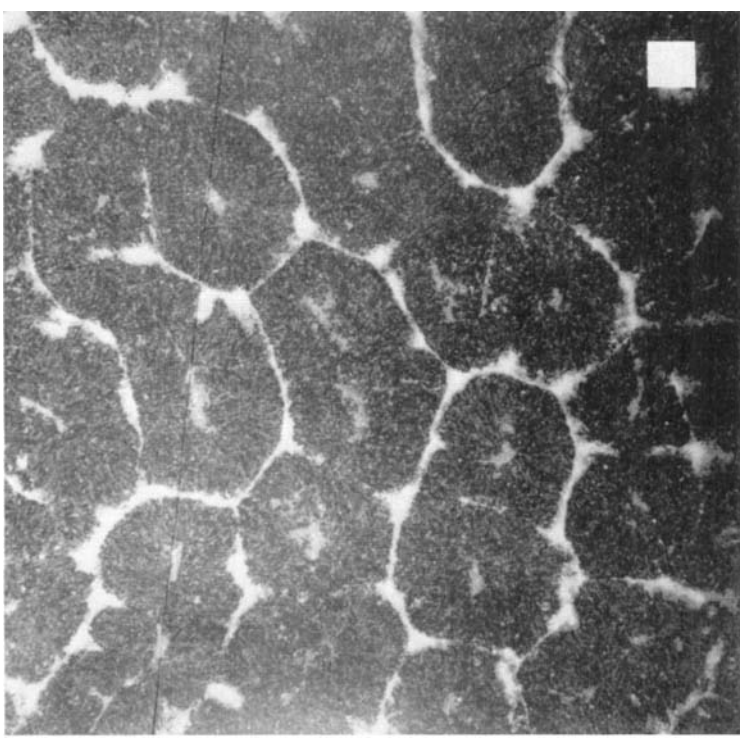

FIGURE 11. Convection pattern at $R/R_c \sim 80$. Main interlinked pattern consists of beads on the bottom; the fainter separate lines are beads on the top.